NASA CONTRACTOR REPORT

NASA CR-2903

NASA CR-2903

TERMINAL ENERGY DISTRIBUTION OF BLAST WAVES FROM BURSTING SPHERES

Andrew A. Adamczyk and Roger A. Strehlow

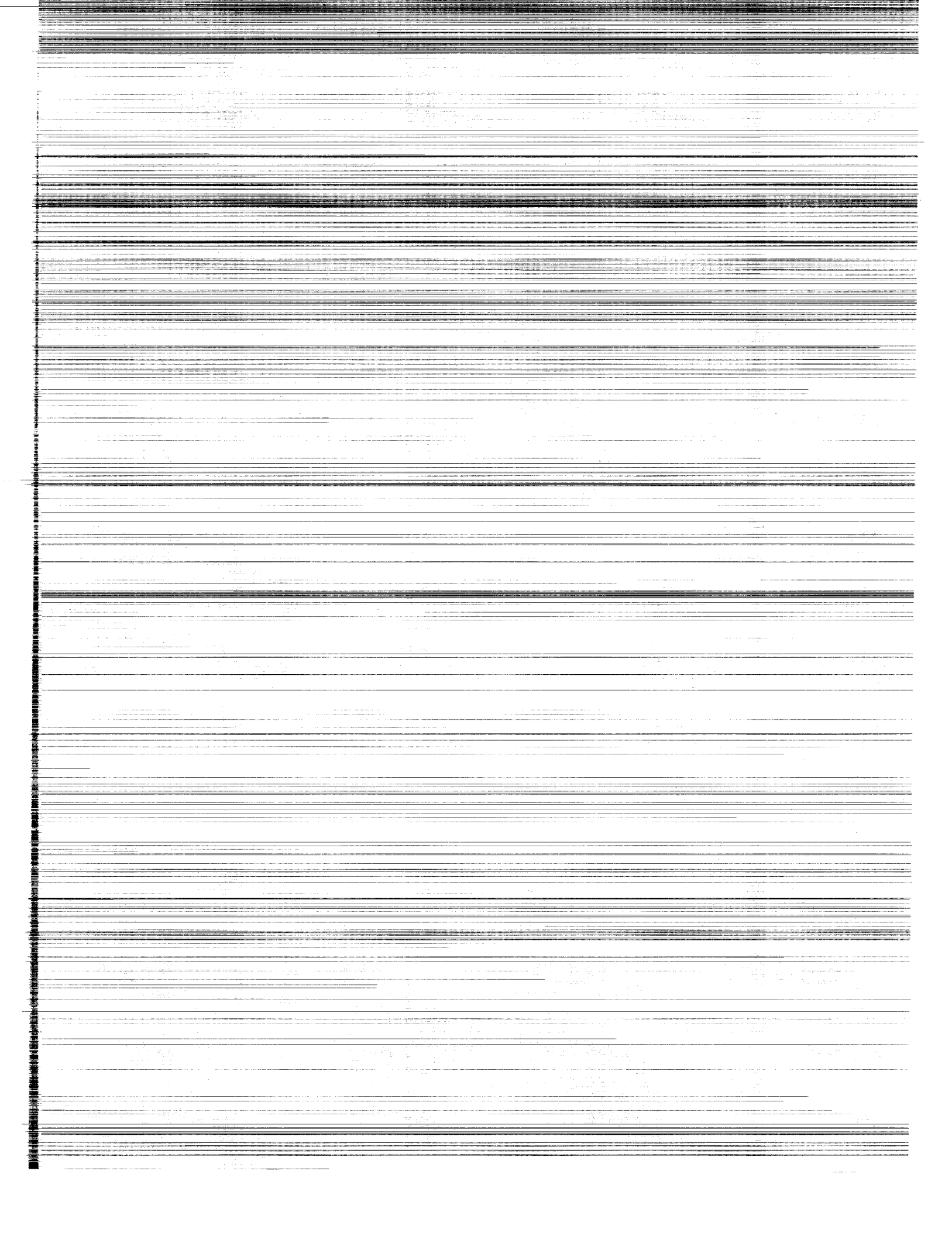NATIONAL AERONAUTICS AND SPACE ADMINISTRATION • WASHINGTON, D. C. • SEPTEMBER 1977

1. Report No. NASA CR-2903	2. Government Accession No.	3. Recipient's Catalog No.
4. Title and Subtitle TERMINAL ENERGY DISTRIBUTION OF BLAST WAVES FROM BURSTING SPHERES		5. Report Date September 1977
		6. Performing Organization Code
7. Author(s) Andrew A. Adamczyk and Roger A. Strehlow		8. Performing Organization Report No. None
		10. Work Unit No.
9. Performing Organization Name and Address University of Illinois at Urbana-Champaign Urbana, Illinois 61801		11. Contract or Grant No. NSG-3008
		13. Type of Report and Period Covered Contractor Report
12. Sponsoring Agency Name and Address National Aeronautics and Space Administration Washington, D.C. 20546		14. Sponsoring Agency Code

15. Supplementary Notes

Final report. Project Manager, Paul M. Ordin, Space Propulsion and Power Division, NASA Lewis Research Center, Cleveland, Ohio 44135

16. Abstract

This report presents the results of the calculation of the total energy delivered to the surroundings by the burst of an idealized massless sphere containing an ideal gas. The logical development of various formulas for sphere energy is also presented. It is shown that for all types of sphere bursts the fraction of the total initial energy available in the sphere that is delivered to the surroundings lies between that delivered for the constant pressure addition of energy to a source region and that delivered by isentropic expansion of the sphere. Furthermore, the relative value of E_s/Q increases at fixed sphere pressure/surrounding pressure as sphere temperature increases because the velocity of sound increases, which allows more work to be performed on the surroundings.

17. Key Words (Suggested by Author(s)) Blast waves; Blast damage; Ideal explosions; Nonideal explosions; Explosions		18. Distribution Statement Unclassified - unlimited STAR Category 28	
19. Security Classif. (of this report) Unclassified	20. Security Classif. (of this page) Unclassified	21. No. of Pages 27	22. Price* $4.00

* For sale by the National Technical Information Service, Springfield, Virginia 22161

Terminal Energy Distribution Of

Blast Waves from Bursting Spheres

by

Andrew A. Adamczyk*

and

Roger A. Strehlow
Aeronautical & Astronautical Engineering Department
University of Illinois at Urbana-Champaign

Introduction

One interesting fundamental property of the blast wave generated by a non-ideal source is the fraction of the energy which is initially in the source region that ends up in the surroundings after the explosion has occurred. For ideal sources, i.e., point source, nuclear or high-explosive explosions, virtually all the source energy ends up in the surroundings. One can relate this to the fact that these are high-energy density and power-density sources. In the case of the ideal burst of a sphere of high-pressure, inert gas, this is not true, however, and the energy imparted to the surroundings can be considerably less than that initially contained in the source region. In this report we will first look at two idealized limit cases, and then use actual pressure-volume-time trajectories calculated for various bursting spheres to deduce a general relationship for the terminal energy distribution of a bursting sphere of ideal gas at high pressure.

---

* Current address, Ford Motor Co., Research Division, Dearborn, Michigan,

Approach:

For any non-ideal explosion, the energy added at the source, Q, eventually partitions itself between the source volume as residual source volume energy, E_B, and the surroundings. The quantity of energy added to the surroundings, E_S, is determined by the work that the source volume does on the surroundings. This work must be evaluated at the contact surface between the source volume and the surroundings, and is given by the path integral

$$E_S = \int_{V_o}^{V_f} PdV \qquad (1)$$

Where P is the instantaneous pressure at the contact surface, V_o is the initial source volume, and V_f is the final source volume that one finds when the system is quiescent, and its pressure has a uniform value, P_o, equal to the external atmospheric pressure.

In each case that we consider, we will assume that both the source volume and surroundings contain an ideal gas which has a constant heat capacity and we will approximate, as appropriate, the actual path integral observed from numerical calculation of the blast wave by a suitable simplified path so as to be able to analytically or numerically evaluate equation 1. In all cases the initial pressure (before energy addition), both in the source volume and in the surroundings, will have a constant value of P_o. However, density, temperature, molecular weight and heat capacity of the source gas may in general be different than that of the surroundings. With these restrictions we consider the following cases:

    I.   Constant pressure addition of energy

    II.   Constant volume addition of energy with subsequent isentropic expansion

    III.   Constant volume addition of energy with the subsequent flow calculated using the equations of motion, (i.e., the bursting sphere).

Case I - Constant pressure energy addition

In this case we assume that energy is deposited homogeneously throughout the source region, i.e., we assume that the rate of energy addition per unit mass within the source volume is the same for all elements of the source volume. Additionally, we assume that the rate of energy addition is <u>very slow</u> - so slow that the pressure remains constant during the energy addition process. With these assumptions, equation 1 may be integrated to yield the equation

$$E_S = P_o \ (V_f - V_o) \tag{2}$$

Furthermore, since the energy is added at constant pressure, the final temperature in the ball is given by the equation

$$T_2 = \frac{Q}{NC_p} + T_1 \tag{3}$$

where N is the number of moles of gas in the source volume, C_p is the constant pressure heat capacity of the gas in the source volume and the subscripts 1 and 2 refer to the initial and final gas temperature in the source volume, respectively. Furthermore, the energy which remains in the source region after Q units of energy have been added is

$$E_B = NC_v \ (T_2 - T_1) \tag{4}$$

and the energy in the surroundings is therefore

$$Q - E_B = E_S = NR \ (T_2 - T_1) = P_o(V_f - V_o) \tag{5}$$

Thus, the fraction of the energy remaining in the source volume after energy addition is

$$\frac{E_B}{Q} = \frac{C_v}{C_p} = \frac{1}{\gamma_1} \simeq 0.714 \text{ for } \gamma_1 = 1.4 \tag{6}$$

and the fraction transmitted to the surroundings is

$$\frac{E_S}{Q} = \frac{R}{C_p} = \frac{\gamma_1 - 1}{\gamma_1} \simeq 0.286 \text{ for } \gamma_1 = 1.4 \tag{7}$$

Here γ_1 is the heat capacity ratio of the gas in the source volume. Notice that the ratios given by equations 6 and 7 are independent of the initial source size, V_o, of the relative energy addition $Q/NC_vT_1 = q$ and of the gamma of the surrounding gas, γ_0. They are only dependent on the heat capacity ratio of the source volume gas. Also note that a majority of the energy remains in the source volume and that no shock wave propagates into the surroundings. This is because the assumption that the energy is added slowly allows acoustic level signals to adjust the position of the surrounding gas as the energy is being added. Furthermore, since the external work was performed at the lowest pressure available to the system, the fraction of energy transferred to the surroundings must be less than that for any other case.

Case II - Constant volume energy addition with subsequent isentropic expansion

For this case, we assume that energy is added instantaneously and homogeneously throughout the source volume at time t = 0, with the source gas expanding isentropically, (i.e., slowly against counter pressure) when t > 0. This energy can be expressed in terms of the state variables of the gas in the

ball using the equation

$$Q = NC_v (T_2 - T_1) = \frac{(P_2 - P_o)V_o}{\gamma_1 - 1} \qquad (8)$$

The right-hand side of equation (8) is Brode's formula [1] for the energy contained in a bursting sphere. Thus, a sphere bursting at a Pressure P_2 and initial temperature T_2 is represented exactly by the instantaneous addition of the quantity of energy Q to a source volume gas which was initially at pressure P_o and temperature T_1. Also note that the stored energy in a bursting sphere is given by $(P_2 - P_o)V_o/(\gamma_1 - 1)$, irrespective of the temperature of the gas in the sphere. However, since $P_o V_o = NRT_1 =$ constant for any specific source volume, the mass of gas in the sphere is inversely proportional to the initial temperature, T_1.

We now assume isentropic expansion of the gases in the source volume against an equilibrium counter-pressure which just matches the source volume pressure at every instant of time. Since the surface pressure is always equal to the internal pressure and since the process is reversible, we obtain the relationship

$$E_S = P_2 V_o^{\gamma_1} \int_{V_o}^{V_f} \frac{dV}{V^{\gamma_1}} = \frac{P_2 V_o}{\gamma_1 - 1} \left[1 - \left(\frac{P_o}{P_2}\right)^{\frac{\gamma_1 - 1}{\gamma_1}} \right] = NC_v T_2 \left[1 - \left(\frac{P_o}{P_2}\right)^{\frac{\gamma_1 - 1}{\gamma_1}} \right] \qquad (9)$$

Equation (9) is identical to that recommended by Baker (2) and Brinkley (3) for determining the energy of a bursting sphere. We now define a useful dimensionless variable

$$q = \frac{Q}{NC_v T_1} = (\gamma_1 - 1) \frac{Q}{P_o V_o} \qquad (10)$$

The quantity q represents the amount of energy that is added to the source volume relative to that initially present in the source volume. Note that

for fixed Q, q can only change if V_o changes, and P, therefore, represents a source energy density. Also note that

$$q = \frac{T_2}{T_1} - 1 = \frac{P_2}{P_o} - 1 \qquad (11)$$

and that, as $q \to \infty$, $V_o \to 0$, and as $q \to 0$, $V_o \to \infty$, at fixed Q and P_o

Manipulating equation (9) and applying the definitions which have been presented, we obtain

$$\frac{E_S}{Q} = \frac{1}{q} \left[(1 + q) - (1 + q)^{1/\gamma_1} \right] \qquad (12)$$

Furthermore,

$$\frac{E_B}{Q} = \frac{NC_v(T_2 - T_1)}{Q} = \frac{NC_v T_1}{Q} \left[\frac{T_2}{T_1} \left(\frac{T_1}{T_2} \right)^{\frac{\gamma_1 - 1}{\gamma_1}} - 1 \right] = \frac{1}{q} \left[(1 + q)^{1/\gamma_1} - 1 \right] \qquad (13)$$

If equations (12) and (13) are added, they show that the total energy, Q, is conserved. Equations (12) and (13) also show that, for isentropic expansion, the fractional energy released to the surroundings is a function of the original source energy density as well as the value of γ_1. If we take the limit of E_S/Q as $q \to \infty$, we obtain

$$\frac{E_S}{Q} \to 1 - q^{-\left(\frac{\gamma_1 - 1}{\gamma_1} \right)} \to 1 \qquad (14)$$

which is the correct point source limit.

However, using L'Hopital's rule in the limit as $q \to 0$, we obtain

$$\lim_{q \to 0} \frac{E_S}{Q} = \lim_{q \to 0} \frac{\{(1+q) - (1+q)^{1/\gamma_1}\}}{q} = \lim_{q \to 0} \frac{1 - \frac{1}{\gamma_1}(1+q)}{1} \to \frac{\gamma_1 - 1}{\gamma_1} \qquad (15)$$

which is equal to the constant pressure energy addition limit. Thus, the

fractional amount of energy that the source volume can contribute to the surroundings varies by about a factor of 4, i.e., from 1 to about .28 for a γ_1 = 1.4 source volume gas.

Case III - The massless bursting sphere initially at high pressure

Using Brode's formula [1] we find that the energy trapped in a bursting sphere is identical to that for instantaneous energy addition as discussed in Case II. We also see that the work performed on the surroundings due to isentropic expansion, as given by Baker's or Brinkley's formula, is always less than the total energy as calculated using Brode's formula. Furthermore, since this idealized expansion is an isentropic reversible process, we would expect the work which is performed on the surroundings to be less for a real sphere burst. This is because at the instant the sphere releases its contents, the contact surface between sphere material and the atmosphere will drop to some lower pressure due to shock wave - rarefaction fan flow-matching at the contact surface. This occurs because in non steady, inviscid flow the momentum equation requires that no pressure gradients can exist unless they are also accompanied by flow velocity gradients. Thus at the instant of burst of the sphere, a rarefaction fan which has both velocity and pressure gradients in it propagates from the edge to the center of the sphere. This causes the gas in the sphere near the boundary to have a lower pressure than the sphere pressure and to simultaneously propagate away from the center. Outside the sphere, in the surrounding gas, the pressure is increased by compression and a shock wave is formed. The flow of the surrounding gas is also away from the center of the sphere. Since the process near the contact surface is quasi steady in coordinates that move with the contact surface, the requirement is that pressure and flow velocity be balanced across that surface at all times. In the spherical case, the pressure at that surface does drop

with time because of flow divergence, but at the very start of the process the region of interest can be assumed to be so thin that divergence is not important and the usual shock wave - rarefaction fan flow matching requirements can be used to calculate the flow velocity and pressure at the instant of burst. Finally, the pressure to be used in equation (1) always remains less than the initial kernel pressure, and may even drop below P_o during portions of the process. However, eventually it must reach P_o as a final state. The exact trajectory can only be calculated using numerical techniques at the present time.

This type of calculation has been performed for a number of cases by Strehlow and Ricker[4]. The output of these calculations was examined to determine the (P,V) behavior with time of the contact surface that separates the sphere contents from the surrounding air. Typical (P,V) trajectories are shown in figures 1 and 2. As can be seen when comparing the isentropic expansion curves to those obtained by integrating the non-steady, gas-dynamic conservation equations, as done in Strehlow and Ricker,[4] the slope of each curve shows a markedly higher value initially and then gradually approaches the isentropic value. This behavior indicates that the effective γ of the gas--the ratio of specific heats which could be used to fit a polytropic pressure-volume curve to the actual pressure-volume curve--has a changing value during the expansion, starting with one which is radically higher from that of the surrounding gas, to one which is approximately equal to that of the surrounding gas. Even though the initial bursting conditions change for the results presented in figures 1 and 2, the general behavior of the slope is consistent. From these results, it can be seen that the expansion process cannot be adequately approximated as a single isentrope, as in case II, and a more detailed evaluation of the expansion process is necessary.

To learn more about the (P,V) behavior of the contact surface, these

data were replotted using log V/Vo and log P/Po as coordinates. Graphs for
eight different initial conditions are shown on figures 3 and 4 as solid
lines. It can be seen that the (P,V) trajectories, even though curved, can
be quite easily approximated as two straight lines in some cases, and as a
single straight line in other cases. A further examination of the flow
associated with the bursting process showed that, for those curves that
showed two slopes, the break in the slope occurred at approximately the
time when the head of the strong inward propagating rarefaction wave
generated at the kernel edge by the burst just reached the contact surface
after reflection from the kernel center. Those cases for which only one
slope was observed were low temperature bursts, in which the sonic velocity
of the kernel gas was very low, and in these cases, the rarefaction fan
did not reach the contact surface before the pressure at the contact
surface reached ambient pressure.

The reason for this (P,V) trajectory with time is not entirely clear
at the present time. The very low initial slope that was observed is obviously
due to the fact that the only flow divergence in spherical coordinates is re-
sponsible for the pressure drop. As will be shown later, the second slope is
very nearly equal to the isentropic exponent for the gas in the sphere and it
will be shown later that if the gas inside the contact surface (the sphere gas)
can be assumed to have a single definable thermodynamic state (which it does
not) this slope should be the isentropic coefficient. This proved to be very
useful in the analysis.

These observations of the numerically-generated pressure-volume curves
have led to a rather simple technique for determing the fraction of the energy
transmitted to the surrounding gas, E_s/Q, for the case of an actual sphere
burst. The technique consists of modelling the actual log pressure-log volume
trace using two straight-line segments when necessary and a single straight-
line segment for the other cases.

The pressure at the kernel edge and the rate of volume change with this pressure is what must be modelled to calculate Es/Q. Figure 5 shows that an expansion fan propagates to the center of the sphere with time, reflects and eventually overwrites the kernel edge. Earlier we stated that for this period of time the (P,V) trajectory is such that it has a straight line behavior on a log P-log V plot with an effective polytropic exponent of k_1 which is considerably smaller than the ordinary polytropic exponent for the gas in the sphere. This is due to the dynamic nature of the expansion process and is a path dependent behavior associated with the initial flow following the busrt of the sphere.

When transformed back into the P-V plane, the straight line relationships (in the log P-log V space) are converted to the expression which is indicative of an ideal polytropic gas

$$\frac{P}{P_0} = \left(\frac{V}{V_0}\right)^{+k_1} = C \tag{16}$$

where $-k_1$ is the slope of the curve in log P-log V space.

Using figure 6 to define the important state points during the expansion process, a simple expression for E_S/Q is derived. Again, from equation 1,

$$E_s = P_0 V_0 \int_1^{V_f/V_0} \frac{P}{P_0} \, d\left(\frac{V}{V_0}\right) \tag{17}$$

From figure 6, it can be deduced that the pressure-volume relationship from state 3 to state 4 can be expressed as

$$\frac{\dfrac{P}{P_0}\left(\dfrac{V}{V_0}\right)^{+k_1}}{\dfrac{P_3}{P_0}\left(\dfrac{V_3}{V_0}\right)^{+k_1}} = 1$$

where or

$$1 \le \frac{V}{V_0} \le \frac{V_4}{V_0} , \qquad 1 \le \frac{V}{V_0} \le \frac{V_f}{V_0} \quad \text{if } V_4 \ge V_f. \tag{18}$$

Here, V_0 is the initial volume of the sphere and P_3 is the pressure at the

contact surface just after the instant of burst and is calculated from the steady state shock-rarefaction fan balance condition. Also, a similar expression can be used for the curve--from state 4 to the point in which ambient conditions are reached. This expression is written as

$$\frac{\dfrac{P}{P_o}\left(\dfrac{V}{V_o}\right)^{k_2}}{\dfrac{P_3}{P_o}\left(\dfrac{V_3}{V_o}\right)^{k_1}\left(\dfrac{V_4}{V_o}\right)^{(k_2-k_1)}} = 1 \qquad (19)$$

where

$$\frac{V_4}{V_o} \leq \frac{V}{V_o} \leq \frac{V_f}{V_o}$$

from equation 19 and the fact that $\dfrac{V_3}{V_o} = \dfrac{P_f}{P_o} = 1$, we obtain

$$\frac{V_f}{V_o} = \left(\frac{P_3}{P_o}\right)^{1/k_2}\left(\frac{V_4}{V_o}\right)^{\frac{k_2-k_1}{k_2}} \qquad (20)$$

which now relates the volume of kernel when it has expanded to ambient conditions to the initial contact surface pressure and the kernel volume when the contact surface is overridden by the reflected rarefaction wave.

To determine this intersection point, point 4, the velocity-time relationship of the rarefaction fan and contact surface must be integrated to obtain the position of each of these boundaries as a function of time until they intersect. In essence, one can obtain an expression for V_4/V_o by integrating the wave propagating speed, u + a, subject to the condition that it propagate from the kernel edge to the origin, reflect and again propagate to the expanding kernel edge.

$$R_e = R_0 = \int_0^{t_1} \frac{dR_1}{dt} \, dt + \int_{t_1}^{t_2} \frac{dR_1}{dt} \, dt \qquad (21)$$

$$R_f = R_o - \int_o^{t_1} a_4 \, dt + \int_{t_1}^{t_2} (\overline{a}_4 + \frac{dR_1}{dt}) \, dt \qquad (22)$$

where R_e is the position of the kernel edge;

R_f is the position of the rarefaction wave;

R_o is the original position of the kernel edge;

$\frac{dR_1}{dt}$ is the velocity of the kernel edge;

$\overline{a}_4$ is the average sound speed at the wave during its propagation.

At the point of intersection, $R_e = R_f$ and

$$\int_o^{t_1} \frac{dR_1}{dt} \, dt = - \int_o^{t_1} a_4 \, dt + \int_{t_1}^{t_2} (\overline{a}_4) \, dt = - a_4 t_1 + \int_{t_1}^{t_2} \overline{a}_4 \, dt$$

$$\qquad (23)$$

$$= - R_o + \int_{t_1}^{t_2} \overline{a}_4 \, dt$$

If $T = t_2 - t_1$ where $\overline{a}_4 \cdot T = \int_{t_1}^{t_2} a_4 \, dt$

then from equation 23

$$T = \frac{R_o + \int_o^{t_1} \frac{dR_1}{dt} \, dt}{\overline{a}_4}$$

R_e at intersection $= R_o + \int_o^{t_1 + T} \frac{dR_1}{dt} \, dt$

$$= R_o + \int_o \left\{ \frac{R_o}{a_4} + \frac{R_o}{\overline{a}_4} + \frac{1}{\overline{a}_4} \int_o^{\frac{R_o}{a_4}} \frac{dR_1}{dt} \, dt \right\} \frac{dR_1}{dt} \cdot dt \qquad (24)$$

and

$$\frac{V_4}{V_o} = \left\{ 1 + \frac{1}{R_o} \int_o \frac{dR_1}{dt} \cdot dt \left[\left\{ \left(\frac{R_o}{a_4} + \frac{R_o}{a_4} + \frac{1}{a_4} \right) \int_o^{\frac{R_o}{a_4}} \frac{dR_1}{dt} \, dt \right\} \right] \right\}^N$$

(25)

Where $N = 1$, 2 or 3, depending on whether the flow field is planar, cylindrical or spherical. However, since no simple solution exists for this truly non-steady flow field, the results of Strehlow and Ricker [4] are used to obtain V_4/V_o.

To determine the amount of energy transmitted to the surrounding gas from state 3 to state 4, equation 18 is substituted into the energy integral presented in equation 17, which yields

$$E_{S_4} = P_o V_o \int_1^{V_4/V_o} \frac{(P_3/P_o) \, (V_3/V_o)^{k_1}}{(V/V_o)^{k_1}} \, d \, (V/V_o)$$

(26)

Furthermore, if one assumes a thermodynamically definable state, the energy which remains in the source region after Q units of energy have been added is

$$E_{B_4} = N_1 C_V \, (T_4 - T_1)$$

(27)

Remembering that the total energy deposited originally in the kernel, Q, equals the sum of the energy transmitted to the surroundings plus the energy remaining in the kernel, and is expressed as

$$Q = E_{B_4} + E_{S_4} = N_1 C_V \, (T_2 - T_1)$$

(28)

Using expressions 26, 27, 28 and the ideal gas law, we obtain

$$\frac{P_4}{P_o} = \frac{\left[\frac{1-\gamma}{1-k_1}\frac{P_3}{P_o}\left(\left(\frac{V_4}{V_o}\right)^{1-k_1} - 1\right) + P_2/P_o\right]}{V_4/V_o} \tag{29}$$

Integrating equation 26 from state 4 to the final state, and summing to the value obtained at state 4, we obtain the energy transmitted to the surrounding gas during the entire process.

$$E_{s_f} = P_o V_o A \left(\frac{V_4}{V_o}\right)^{(1-k_1)}\left[\frac{1}{1-k_1} - \frac{1}{1-k_2}\right] - \frac{P_o V_o A}{1-k_1} + \frac{P_o V_o A}{1-k_2}\left(\frac{V_4}{V_o}\right)^{(k_2-k_1)}\left(\frac{V_f}{V_o}\right)^{(1-k}\tag{30}$$

where $A = P_3/P_o$.

Again assuming a thermodynamically definable end state, the energy remain in the kernel can be expressed as

$$E_{B_f} = N_1 C_V (T_f - T_1) \tag{31}$$

and

$$E_{s_f} = \frac{N_1 R}{\gamma - 1} (T_2 - T_f) \tag{32}$$

Using the ideal gas law, equation 32 can be expressed as

$$\frac{E_{s_f}}{P_o V_o} = \left(\frac{P_2}{P_o} - \frac{V_f}{V_o}\right)\frac{1}{\gamma-1} \tag{33}$$

and solving for V_f/V_o, we obtain

$$\frac{V_f}{V_o} = (1 - \gamma) \frac{E_{s_f}}{P_o V_o} + \frac{P_2}{P_o} \tag{34}$$

substitution of equation 30 into equation 34 yields the following expression for the final volume.

$$\frac{V_f}{V_o} = (1-\gamma) \left[A\left(\frac{V_4}{V_o}\right)^{1-k_1} \left[\frac{1}{1-k_1} - \frac{1}{1-k_2}\right] - \frac{A}{1-k_1} + \frac{A}{1-k_2}\left(\frac{V_4}{V_o}\right)^{k_2-k_1}\left(\frac{V_f}{V_o}\right)^{1-k_2}\right] + \frac{P_2}{P_o} \tag{35}$$

and substituting equation 20 yields

$$A^{1/k_2} \left(\frac{V_4}{V_o}\right)^{\frac{k_2-k_1}{k_2}} \left[\frac{\gamma-k_2}{1-k_2}\right] = (1-\gamma) \left[\left(\frac{V_4}{V_o}\right)^{1-k_1} \frac{k_1-k_2}{(1-k_1)(1-k_2)} - \frac{1}{(1-k_1)}\right] A + \frac{P_2}{P_o} \tag{36}$$

using expressions 18 and 29, we obtain

$$\frac{P_2/P_o}{P_3/P_o} = \left[\left(\frac{V_4}{V_o}\right)^{1-k_1} \cdot \frac{\gamma-k_1}{1-k_1} + \frac{1-\gamma}{(1-k_1)}\right] \tag{37}$$

This expression, used in conjunction with equations 25, 36 and 38 (as obtained from Liepman and Roshko [5])

$$\frac{P_2}{P_o} = \frac{P_3}{P_o} \left(1 - \frac{(\gamma_2-1)(a_o/a_2)(P_3/P_o-1)}{\sqrt{2\gamma_o}\sqrt{2\gamma_o+(\gamma_o+1)(P_3/P_o-1)}}\right)^{\frac{-2\gamma_2}{(\gamma_2-1)}} \tag{38}$$

where γ_2 is the ratio of specific heat of the gas initially in the kernel, yields values for k_1, k_2, and V_4/V_o. Then applying equation 30, the energy

to the surrounding gas is calculated.

In these calculations, it can be seen that the u + a field within the kernel is of primary importance, since it explicitly determines the fraction of total energy available to the shock wave. Furthermore, if the sound speed in the kernel is very low, the rarefaction wave does not override the kernel edge before the pressure at the edge has been reduced to the pressure of the surrounding gas. In this case, there is no abrupt change in slope of the log P-log V curve and $k_1 = k_2$ for the entire process. For this special case, equation 36 reduces to

$$A^{1/k_1} \left[\frac{\gamma - k_1}{1 - k_1} \right] = (1 - \gamma) \left[\frac{-A}{1 - k_1} \right] + \frac{P_2}{P_0} \tag{39}$$

Using this expression, equation 38 and equation 30 with $k_1 = k_2$, the energy transmitted to the surrounding gas is calculated.

It should be noted that, since state 4 and the final end state were assumed to be thermodynamically definable in this model, k_2 is equal to γ along this segment of the P-V curve. Furthermore, one can observe in figure 3 that the slope of this segment of the actual pressure-volume curves does indeed have a value very nearly equal to the γ of the surrounding gas.

Results and Conclusions

Using both the single-line and double-line theories to evaluate the
fraction of energy transmitted to the surrounding gas, values of E_S/Q for
each of the log P/P_0 - log V/V_0 curves in figure 3 are plotted in figure 7
versus the initial pressure ratio in the sphere. The smooth curves were
calculated using single line theory for T_4/T_0 = 0.5, 50, and 5000 and using
double line theory for T_4/T_0 = 50. These curves are compared to the
theoretical values for case 1 (constant pressure addition of energy,
E_S/Q = 0.286) and for case 2 (isentropic expansion against counter pressure).
They are also compared to the results of Strehlow and Ricker.[4] It should
be noted here that $P_2/P_0 - 1 = q$, the energy density of the sphere gas.

Notice the large scatter in the results of the Strehlow and Ricker
calculations. Some of this scatter, particularly the lower values of E_S/Q
obtained from some runs is due to the fact that for these cases, the cal-
culation was not carried out long enough to obtain terminal values. It
can be noted on figures 3 and 4 that some calculations were terminated when
the interface pressure was well above atmospheric. The remaing scatter is
probably due to the late time accumulation of numerical errors.

The T_4/T_0 = 0.5 curve on figure 7 should represent the actual terminal
energy distribution, because for these initial conditions the behavior is
well approximated by a single line curve. The T_4/T_0 = 50 cases on figure
7 should not agree with the single line calculation because the reflected
rarefaction wave will reach the contact surface well before the contact
surface pressure drops to P_0. Thus it is not surprising that the Strehlow
and Ricker values show better agreement to the double-line theory than to
the single-line theory.

Finally, it should be noted from figure 7 that the values of E_S/Q for
a bursting sphere, as predicted by this relatively simple theoretical approach,

all lie between the Case I and Case II limit values. Furthermore, at fixed
sphere energy density, $q = P_2/P_0 - 1$, as T_4/T_0 ranges from zero to infinity
the E_s/Q value ranges from the constant pressure limit to the isentropic
limit. This is as it should be because if the temperature in the sphere
is very low, the velocity of sound approaches zero and the contact pressure
approaches P_0. On the other hand, if the temperature in the sphere approaches
infinity, the velocity of sound becomes very large and the expansion is as
an isentropic expansion at the contact surface because the sphere pressure
is spatially uniform at all times during burst. Thus we have shown that
the E_s/Q value for all bursting sphere cases lie between the constant pres-
sure addition case, in which no shock is transmitted to the surroundings
and the isentropic case in which the maximum work is being performed on
the surroundings.

References

1. H. L. Brode, "Blast Wave from a Spherical Charge," Physics of Fluids, 2, 217 (1959)

2. W. E. Baker, "Explosions in Air," University of Texas Press, Austin, Texas (1973) pp. 26.

3. S. R. Brinkley, "Determination of Explosion Yields," AICHE Loss Prevention, 3, 79-82 (1969).

4. R. A. Strehlow and R. E. Ricker, "The Blast Wave from a Bursting Sphere," AICHE Loss Prevention, 10, 115-121 (1976).

5. H. W. Liepman and A. Roshko, "Elements of Gas Dynamics," Wiley and Sons, New York, (1957), p. 81.
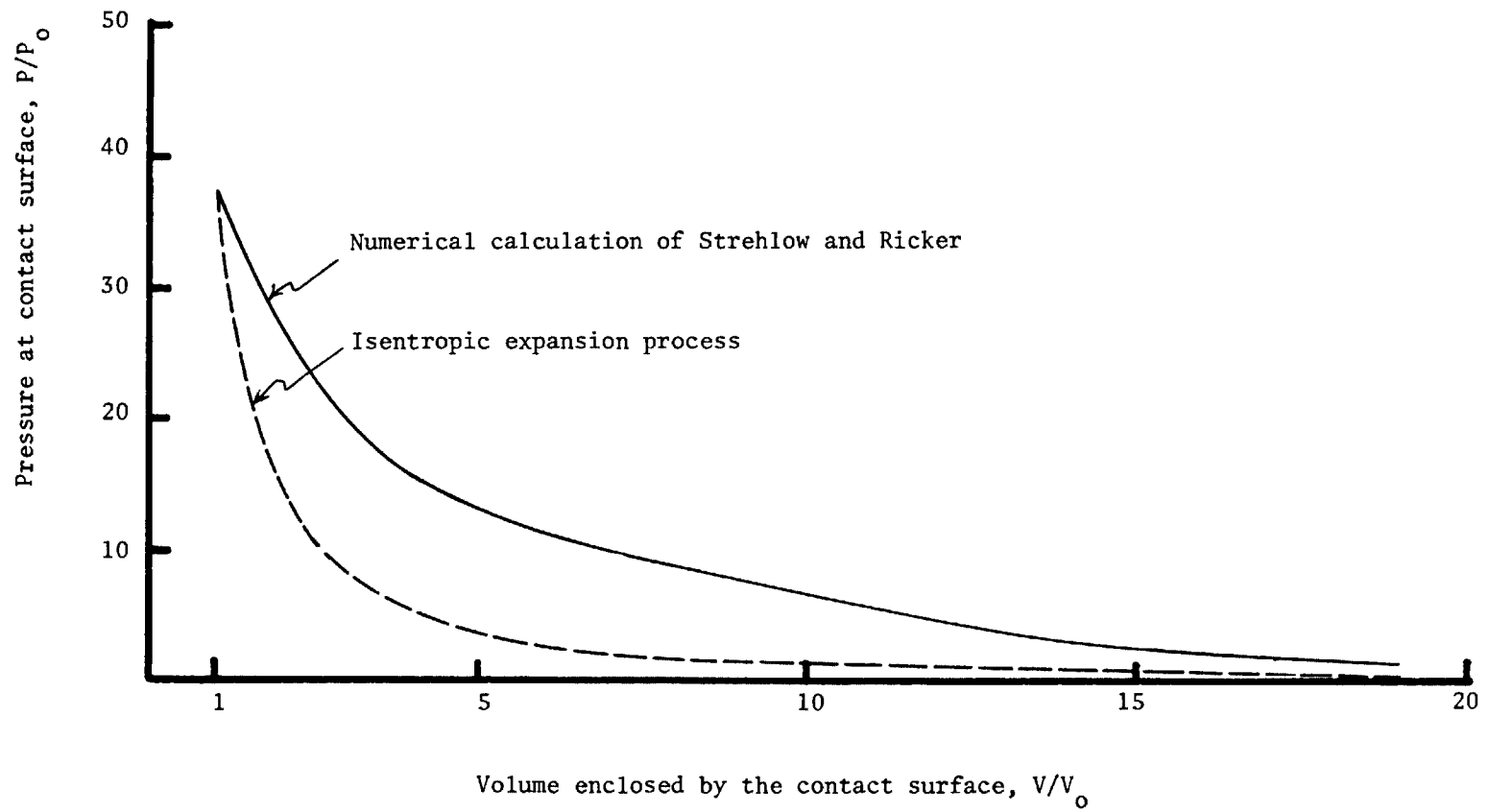
Figure 1. Pressure-volume behavior at contact surface for a typical bursting sphere (Hot sphere; $P_4/P_o = 100$, $T_4/T_o = 50$).
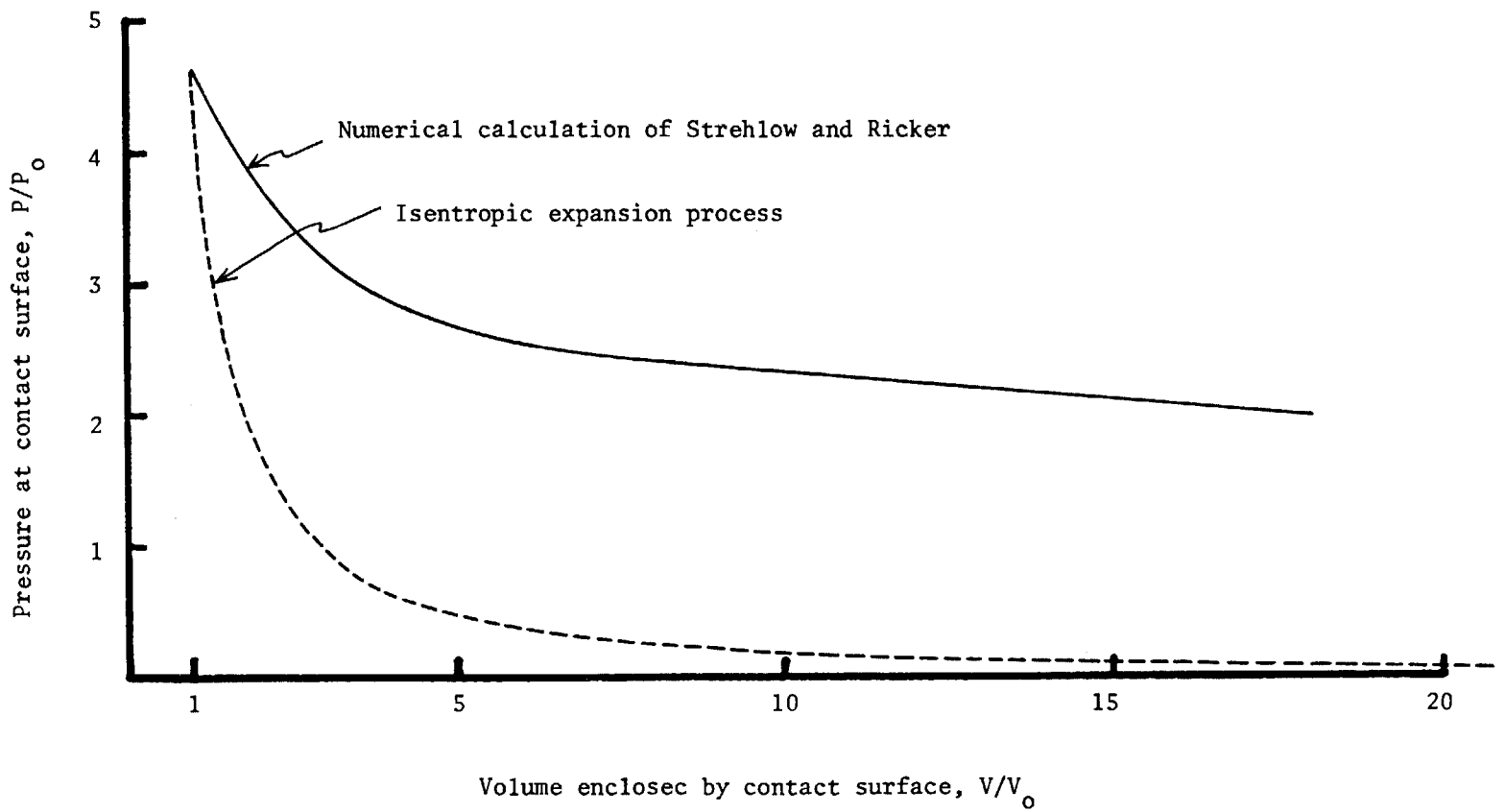
Figure 2. Pressure volume plot at the contact surface for bursting sphere, (cold sphere; $P_4/P_o = 100$, $T_4/T_o = 0.5$).
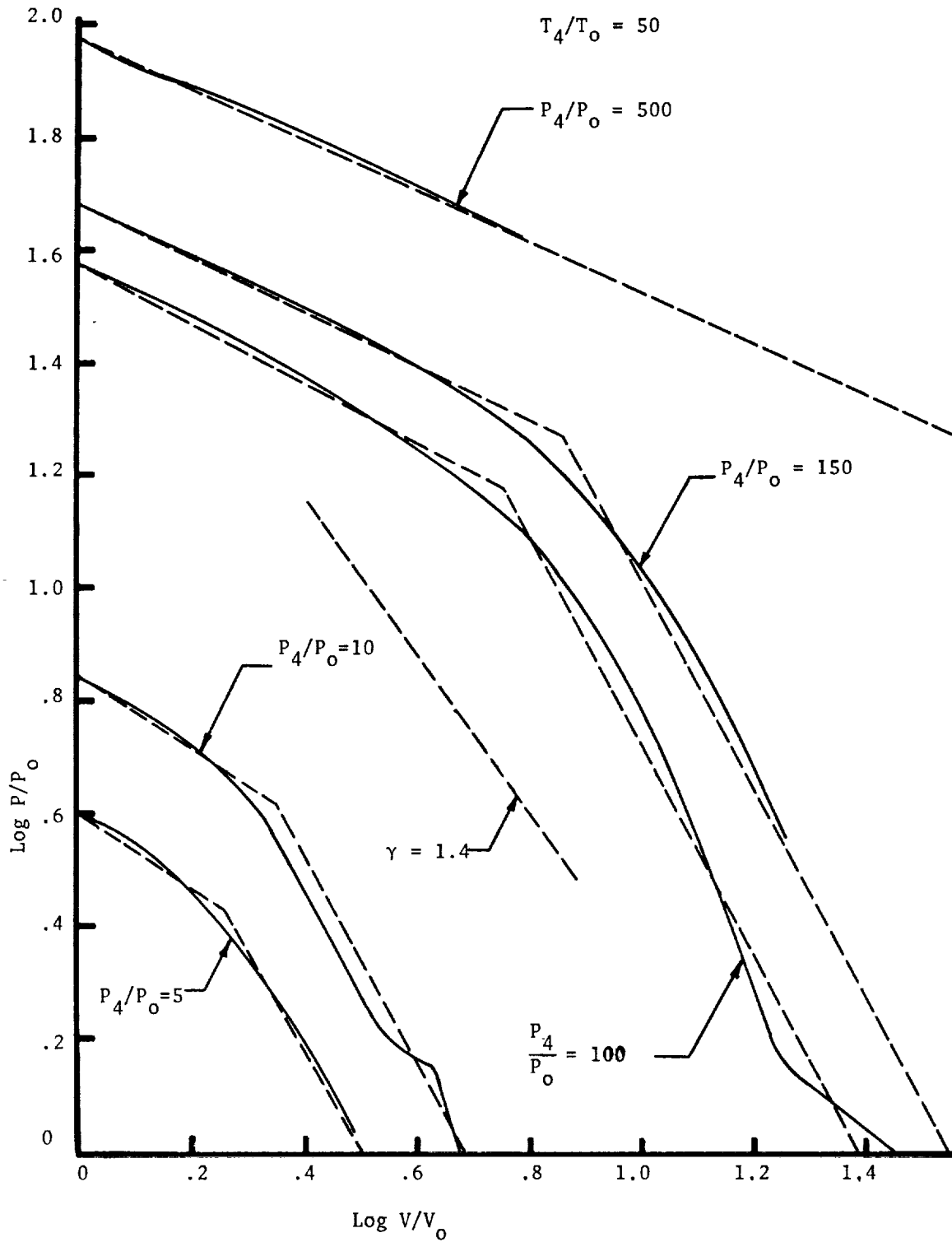
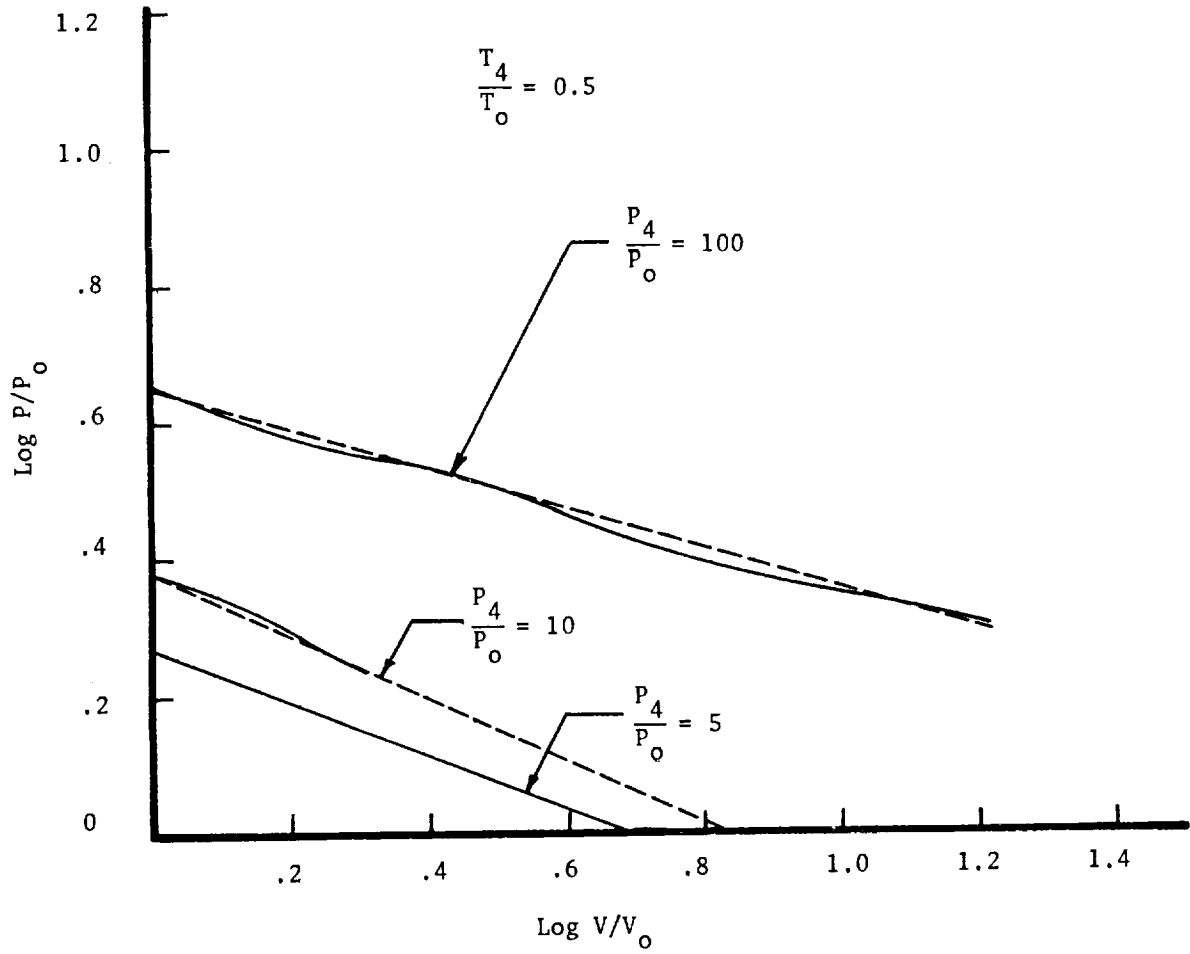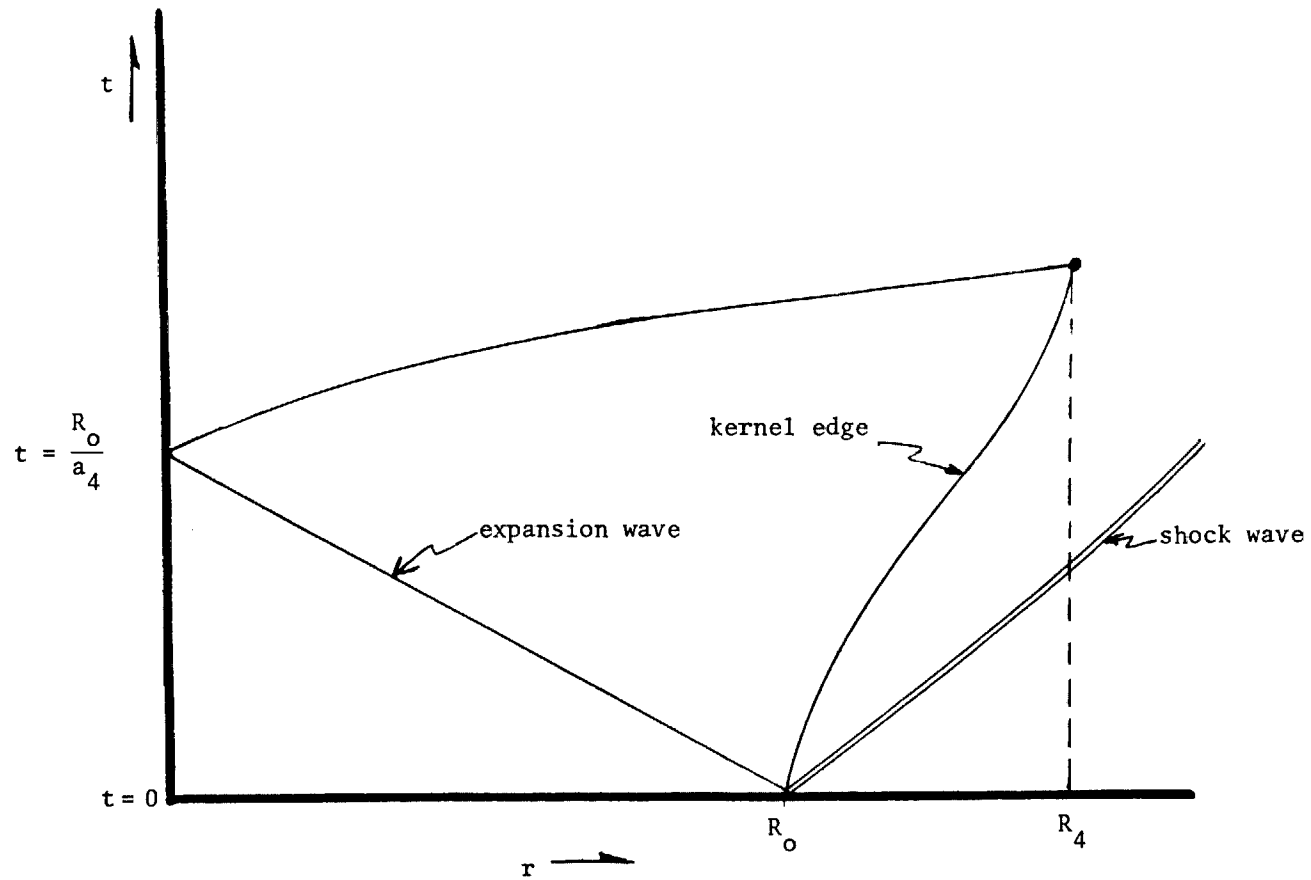Figure 3. Plot of pressure-volume at the edge of an expanding explosive kernel (Hot spheres; $T_4/T_o = 50$).

Figure 4. Plot of pressure-volume at the edge of an expanding explosive kernel (cold spheres; $T_4/T_0 = 0.5$).

Figure 5. Schematic representation of the path the expansion wave travels before encountering the kernel edge.
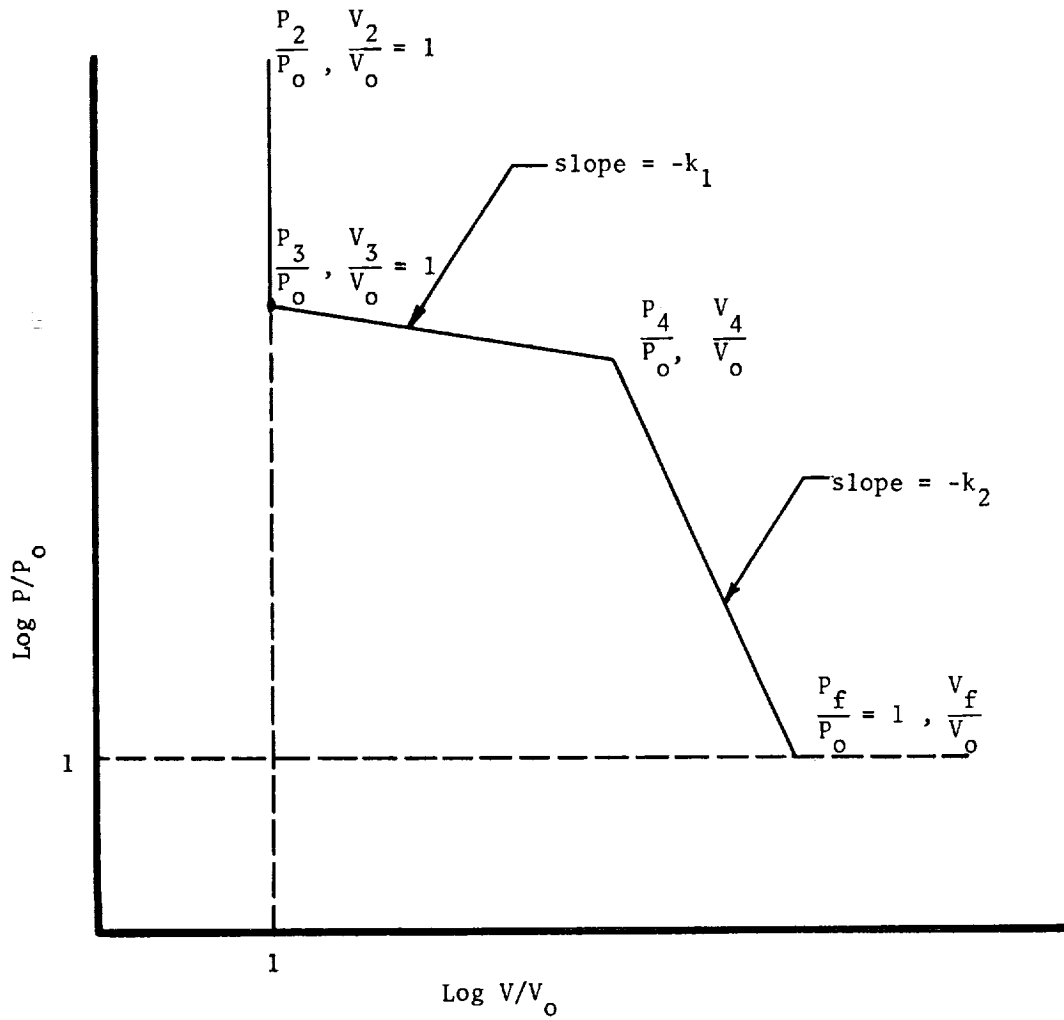
Figure 6. Schematic of the model chosen to represent the contact
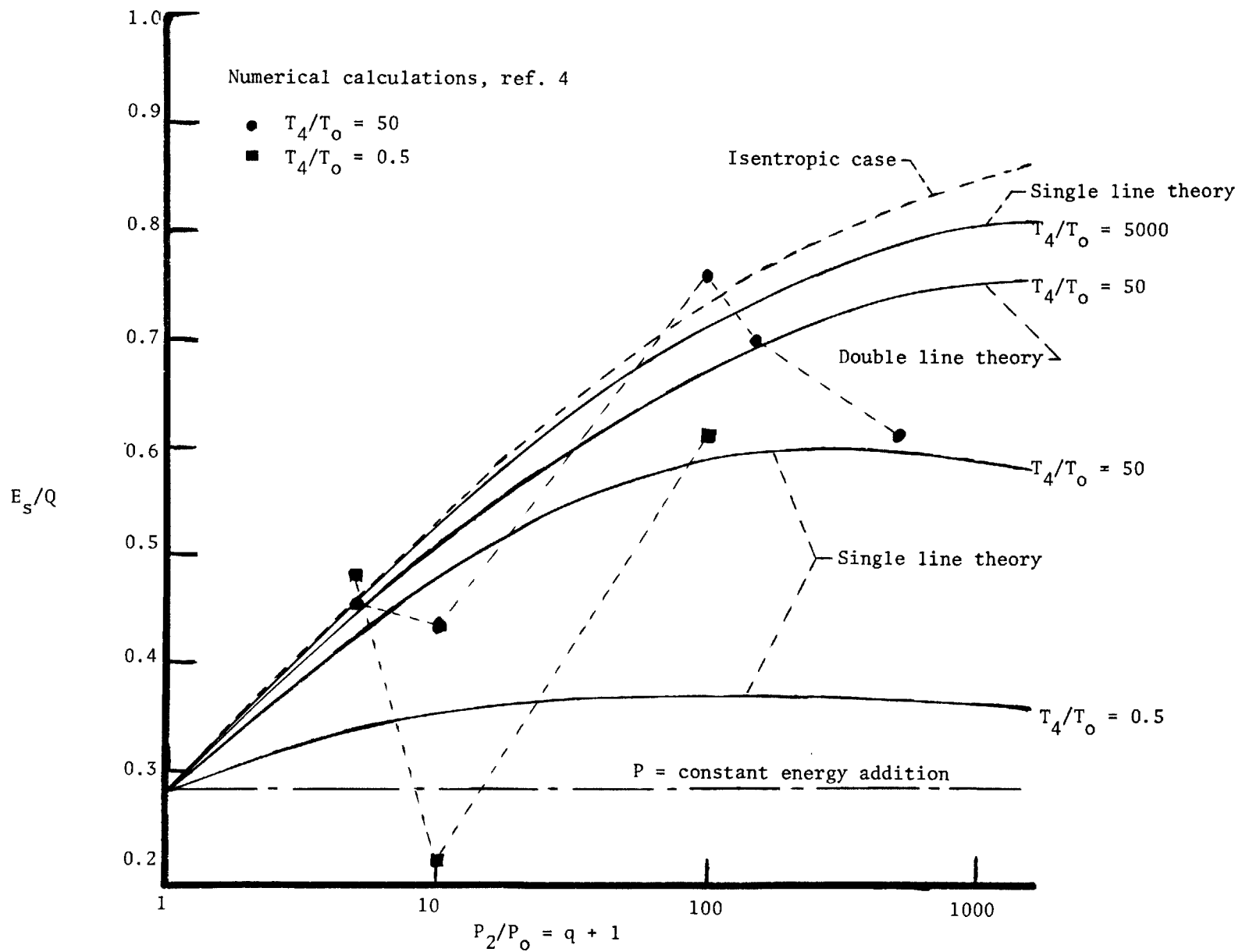surface log pressure - log volume curve of a bursting
sphere.

Figure 7. Summary of results. Terminal values of E_s/Q versus P_2/P_o for different bursting spheres.